2003-01-1064

Optimization of the Combustion Chamber of Direct Injection Diesel Engines

Arturo de Risi, Teresa Donateo and Domenico Laforgia
Università di Lecce –Dipartimento di Ingegneria dell'Innovazione, 73100 via Arnesano, Lecce – Italy

ABSTRACT

The optimization procedure adopted in the present investigation is based on Genetic Algorithms (GA) and allows different fitness functions to be simultaneously maximized. The parameters to be optimized are related to the geometric features of the combustion chamber, which ranges of variation are very wide. For all the investigated configurations, bowl volume and squish-to-bowl volume ratio were kept constant so that the compression ratio was the same for all investigated chambers. This condition assures that changes in the emissions were caused by geometric variations only. The spray injection angle was also considered as a variable parameter.

The optimization was simultaneously performed for different engine operating conditions, i.e. load and speed, and the corresponding fitness values were weighted according to their occurrence in the European Driving Test. The evaluation phase of the genetic algorithm was performed by simulating the behavior of each chamber with a modified version of the KIVA3V code. The parameters for the sprays and the combustion models were adjusted according to the experimental data of a commercial chamber geometry taken as baseline case. Three fitness functions were defined according to engine emission levels (soot, NOx and HC) and a penalty function was used to account for engine performance.

The goal of the optimization process was to select a chamber giving the best compromise of the selected fitness functions. Furthermore, chambers optimizing each single fitness function were also analyzed. The influence of the geometric characteristics on emissions has also been investigated in the paper.

INTRODUCTION

In direct injection diesel engines for automotive application, the combustion chamber is usually characterized by a re-entrant toroidal bowl piston with a protuberance in the bottom of the chamber and a multi-hole nozzle to improve air-fuel mixing.

This type of combustion system was firstly introduced in 1934 by a Swiss company named Adolph Saurer. Saurer claimed the invention of a centrally disposed combustion space separated by the power cylinder but communicating with it by a reduced opening, in order to throttle the air passing from the power cylinder to the combustion space [1]. This combustion space was of annular shape with an approximately circular cross section. In the same patent application [1], Saurer also claimed the introduction of a wart-like protuberance in correspondence of the cylinder axis in order to produce the helical motion of the charging air. This combustion chamber typology was after adopted by several companies, like Fiat, Scania, Volvo, PSA, British Leyland and many others.

To apply direct injection combustion systems to medium-to-small diesel engines, a high swirl combustion chamber was developed and patented by the German company Maschf Augsburg Nuerberg (M.A.N) [2, 3]. The M.A.N. combustion system consisted of a quite deep hemispherical bowl and a single-hole nozzle whose spray was oriented tangentially to the bowl wall in order to increase air-fuel mixing.

With the introduction of high pressure injection systems, a satisfactory air-fuel mixing could be obtained without adopting M.A.N.-like combustion chambers and open or slightly reentrant toroidal chambers were used for automotive application. Thanks to their higher combustion efficiency and low emissions levels, cars equipped with direct injection diesel engines and Common Rail injection systems are now widely diffused in the European automotive market and a great support has been given to research in order to optimize both injection systems and combustion chamber shape.

Moreover, the development of CFD codes for engine simulations and the use of high performance computers allowed researchers to overcome the limitation of experimental investigation. In fact, only a small number

of chamber shapes can be contemporary analyzed and compared with experimental studies, while a wide parametric study can be easily performed with the use of simulation codes.

From results in literature, Heywood [4] deduced that for a fixed compression ratio, the swirl levels at TDC increases if the bowl diameter is reduced, leading to less smoke, higher NO_x levels and HC emissions. The squish-swirl interaction, instead, is influenced by the offset of the bowl with respect to the cylinder axis.

In 1990 Tsao, Dong e Xu [5] used the KIVA-II code to analyze the influence of the bowl depth on the flow field in the case of open toroidal combustion chambers. They found that, in the case of deep combustion chambers, the fuel velocity in the center of the chambers is increased due to the higher inertia. They also stressed the positive effect of the higher clearance on the squish motion and so, on the fuel distribution.

In 1995 Zhang et al. [6] studied the influence of combustion chamber geometry on flame speed by considering three different chamber shapes for a large bore diesel engine equipped with a low-pressure injection system. They found that adopting a re-entrant chamber, the combustion is enhanced during the expansion stroke, preventing the diffusion of the flame in the squish region and giving lower smoke levels. As far as the mean combustion velocity is concerned, it increases with the combustion chamber radius and is lower in the case of flat-bottom bowls.

More recently Bianchi et al. [7] showed that high pressure common rail injection systems provide sufficient mixing also with slightly re-entrant bowl and a low swirl level.

Reitz and his research group applied a computer code (KIVA-GA) to optimize the combustion chamber geometry together with several engine input parameters (e.g. EGR, injection profile, etc.) [8-10]. In those studies, the bowl geometry was defined by three input variables (bowl diameter, bowl depth and central crown height of the piston) allowing only open chamber profiles to be investigated. Moreover, the larger number of parameters included in the GA optimization makes the interpretation of results quite complicated preventing straightforward interpretation of the effect of combustion chamber geometry on engine performance and emissions.

The effect of combustion chamber shape on the engine performance is very complex due to its influence on the flow field and the air-spray interaction and the results in literature confirm that it is difficult to define an optimized combustion chamber, because of the influence of engine specification and injection system. Moreover, De Risi et al. [11] found that the effect of the bowl shape on emissions levels depends on engine load conditions. Thus, combustion chamber optimization should be performed for different operating conditions. Senecal et al. [12] applied the KIVA-GA optimization method to optimize chamber for two operating modes. The grid generator used by Senecal permits a large variety of shapes, but the results presented in [12] are unsuitable for practical application.

The aim of the present investigation is to illustrate an innovative methodology based on genetic algorithms to optimize combustion chamber geometry. This method differs from others available in literature because it takes into account different operating conditions (i.e., load and speed values). Moreover, the optimization method presented here allows several objectives to be contemporary optimized and the outcome of the optimization process is twofold. On the one hand, the method is designed to search for a chamber better than the baseline case with respect to all goals and for all selected operating conditions. On the other hand, the results of the process define the whole Pareto's front so that also chambers giving the best performance according to each objective are obtained. This is very important to understand the effect of combustion chamber geometry on NO_x emissions, soot levels and engine performance for different values of speed and load.

The method has been applied to the optimization of a small bore direct injection diesel engine. The selected operating conditions were achieved with a single injection strategy and no EGR, to avoid that the influence of changes in chamber geometry be masked by the effect of engine control parameters, like injection profile and timing, EGR, boost pressure.

THE MULTI-OBJECTIVE GENETIC ALGORITHM

In the present investigation, the optimization process was performed with a multi-objective genetic algorithm already tested by the authors and applied to engine optimization problems [14-16].

The algorithm starts from a random initial population of binary strings, which codifies a combination of parameters to be evaluated. Then, the algorithm calculates the fitness of each individual according to each single objective to be optimized and individuals are ranked according to Pareto optimality criterion. According to Pareto optimality, a vector **x** is partially less (<p) than **y** when:

$$x < y \iff \forall i \ (x_i \le y_i) \wedge \exists i \ (x_i < y_i) \qquad (1)$$

If the condition (1) is verified, **y** is said to dominate **x**. If a vector is not dominated by any other, it is said non dominated or not inferior.

To describe the application of this criterion to a multi-objective problem, the following example can be useful. With reference to Figure 1, points A – E can be considered as representative of 6 individuals of an optimization process aiming at maximizing two objective functions f_1 and f_2 reported on the axes. Points E, C and

D can be said “non dominated” according to eq.(1). Moreover, each individual A – E can be ranked by considering the number of individuals by which it is dominated, increased by one. Thus, the non dominated individuals (E, C, D) of figure 1 have rank equal to 1 (non dominated points), B and F have rank equal to 2 and 3, respectively and point A, being dominated by all other points, has rank equal to 6. The overall fitness of individual *j* has been calculated according to its rank by using equation (3).

$$F_R(j) = \exp(1 - r(j)) \qquad (2)$$

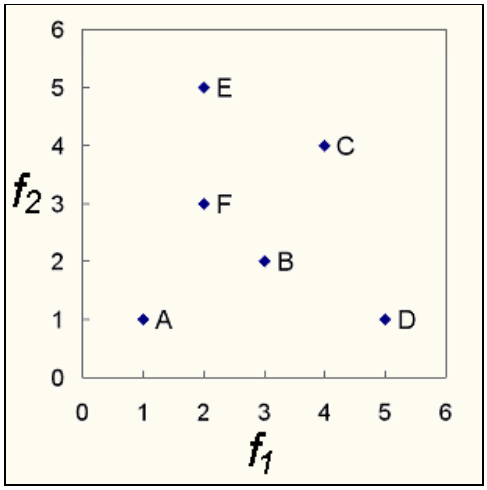

Figure 1 –Example of multi-objective optimization

The best individuals, i.e. the strings with high overall fitness values, are selected for reproduction with the tournament method and their chromosomes are exchanged with the single point crossover technique. The elite strategy is performed by replacing some strings from the new population with individuals extracted from the set of Pareto optimal solutions of the previous generation (non dominated individuals). The new generation is used as starting generation and all the above phases are repeated [13].

To achieve a wider diversity a large number of individuals (50-100) in the population or a micro-Ga (μGA) approach should be used. A typical micro-GA technique uses a very small number of individuals for generation and search for the convergence of individuals towards an unique binary string, i.e. the local optimum. In the present investigation, the two strategies have been compared.

THE KIVA 3V CODE

Numerical simulations were performed by using a modified version of the KIVA 3V code [17]. The improved models for spray, turbulence, combustion process and emissions mechanisms of formation are recalled here, while a complete description of the models can be found in [18]. The modified RNG k-ε model proposed by Han et al. [19] has been used to simulate the in-cylinder turbulent flow field. The fuel injection process is modeled by using the blob injection model [17]. A breakup model based on the Kelvin-Helmholtz and Reyleigh-Taylor instability criteria has been chosen to describe the drop break-up process after injection [20]. The autoignition process is simulated with the Shell model [21], while the combustion chemistry is modeled with the laminar and turbulent characteristic time combustion model proposed by Abraham et al. [22]. The combustion model is activated when a threshold temperature of 1100 K is reached or a determined amount of combustion products is generated by the ignition process. The soot emission model adopted in the present study is the Hiroyasu formation model [23] combined with the Nagle and Strickland-Constable oxidation model [24]. NO emissions are modeled with the Zel’dovich mechanism. All spray models have been adapted so that fuel density is allowed to change according to drop temperature and local pressure, as reported in [25].

THE OPERATING CONDITIONS

The operating conditions (i.e. load and speed values) for engine optimization were selected to minimize the emissions of the most recurring modes in the global European Driving Test, consisting of four urban (ECE) and one extra-urban (EUDC) cycles.

By using the transmission ratios of a five gears compact car, vehicle velocity was correlated to engine speed and the corresponding engine torque was computed by estimating the rolling and aerodynamic resistances of the car, *F*, according to eq. (3).

$$F = F_0 + F_1 \cdot V^2 \qquad (3)$$

where forces are in Newton and V is the vehicle speed in km/h; for this investigation, the values F_0=190 N and F_1=0.0034 N/(km/h)^2 were set.

The most recurring operating modes resulting from such an analysis are reported in Table 1, as mode 1 and 2, while mode 3 was selected to check engine performance at high speed conditions. The operating conditions for the three modes are reported in Table 1.

The optimization was carried out using as reference a commercial small-bore diesel engine whose characteristics are reported in Table 2. The combustion chamber of this engine was chosen as the baseline shape and experimental data were used to set the numerical and physical parameters required by the simulation code.

Mode	1	2	3
Engine speed [rpm]	1500	2000	4000
Injected mass [mg]	10.5	17.5	38.0
Injection start [CA BTDC]	2.4	5.2	7.5
Injection duration [CA]	8.0	9.2	35.0

Table 1 – Operating conditions

Bore [mm]	78.38
Stroke [mm]	86.4
Connecting rod length [mm]	158
Compression ratio	17.2
Inlet Valve Closing [CA BTDC]	134
Injection system	Common Rail
Number of holes	6
Holes diameter [μm]	145

Table 2 – Engine specifications

COMBUSTION CHAMBER PARAMETERIZATION

In order to analyze a wide range of combustion chamber shapes, a parametric grid generator has been developed. For each combination of the five geometric parameters of Figure 2, the program calculates a chamber profile so that the bowl volume equals the reference value (18 cc) to preserve the same compression ratio and squish region volume. Then, the computational grid is generated with a number of divisions along x and z axes giving the same cell size for all the investigated meshes.

The spray angle (θ) was also considered in the optimization process because it influences the interaction between flow field and spray in the combustion chamber.

Note that the grid generator reproduces the baseline combustion chamber using the parameters reported in Table 3. In this table, the range of variation allowed to each parameter is also reported. A resolution of 16 steps was used for all parameters.

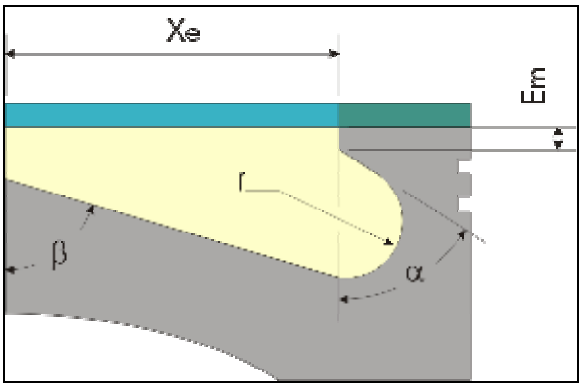

Figure 2 – Combustion chamber definition

Parameter	Baseline value	Range of variation
x_E [mm]	21.03	15-34
α	51.78	-90° – 90°
β	67.43	45° – 135°
r [mm]	5.5	2.0-14.0
e_m [mm]	2.85	1.0-5.0
θ	80°	50° - 80°

Table 3 – Parameters range of variation and baseline values

OPTIMIZATION PROCESS

For the optimization process, three single fitness functions were defined according to engine emissions for modes 1 and 2 of Table 1. In particular, NO_X, soot and HC levels were predicted for each chamber by numerical simulation, compared with the baseline chamber emission values, and then weighted as follows:

$$F_1 = w_{\text{mode1}}\left(\frac{(NO_x)_0}{NO_x}\right)_{\text{mode1}} + w_{\text{mode2}}\left(\frac{(NO_x)_0}{NO_x}\right)_{\text{mode2}} \quad (4)$$

$$F_2 = w_{\text{mode1}}\left(\frac{(soot)_0}{soot}\right)_{\text{mode1}} + w_{\text{mode2}}\left(\frac{(soot)_0}{soot}\right)_{\text{mode2}} \quad (5)$$

$$F_3 = w_{\text{mode1}}\left(\frac{(HC)_0}{HC}\right)_{\text{mode1}} + w_{\text{mode2}}\left(\frac{(HC)_0}{HC}\right)_{\text{mode2}} \quad (6)$$

where the subscript 0 is referred to the base line case and w_{mode1} and w_{mode2} represent the weight assigned to modes 1 and 2 according to their emission contribution in the European Driving Test. From this consideration, a value of 0.5 was set for both modes because the total emission levels of the two modes were about the same.

Moreover, a penalty function, defined as in Figure 3, was used to reduce chamber fitness values when the predicted IMEP was lower than the baseline value.

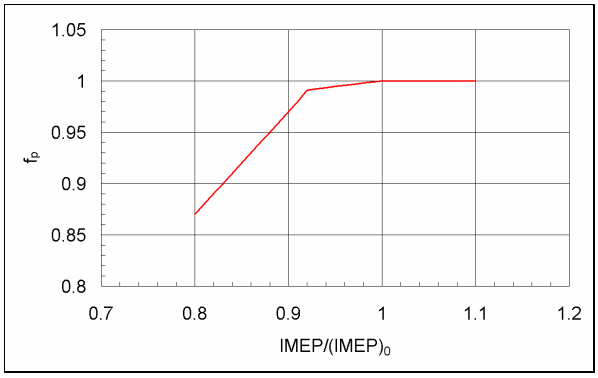

Figure 3 – Penalty function

To reduce the computational time only the closed-valves portion of the engine cycle is simulated and simulations are stopped at 60° ATDC.

RESULTS OF THE OPTIMIZATION PROCESS

The results of the optimization process are shown in Figure 4, as points in the plane F_1-F_2, (i.e, the fitness functions defined according to NO_x and soot emissions, respectively). Since the fitness values F_1 and F_2 have been already scaled by the penalty function, the chambers selected in the optimization process are expected not to reduce IMEP significantly. As far as HC emissions are concerned, almost all the chambers lying

on the Pareto's front exhibit a reduced level of unburned hydrocarbons with respect to the baseline case. Therefore, the choice of the best combustion chamber configurations can be performed by analyzing the results in the plane F_1-F_2.

COMPARISON BETWEEN STANDARD- AND MICRO-GAs PERFORMANCE

Results of Figure 4 show also a comparison between a standard-GA with 50 individuals for generation and a micro-GA with 5 individuals. In particular, the results obtained with the micro-GA are reported as black rhombs while the individuals selected by the standard-GA are marked with empty circles. Configurations A, B, C, D, E, which define Pareto's front, belong to the set of results obtained with the standard genetic algorithm. The total number of generations was set equal to 250 and 25 for the micro-GA and the standard GA, respectively, so that the computational evaluations were the same for both cases. Note that the standard-GA allows a slightly better definition of Pareto's front to be obtained with respect to the micro-GA. This does not confirm the results found by Carroll [13] in the case of single objective optimization, and the test performed by the authors in a previous investigation [15] where the comparison has been carried out in the case of only two-objective functions.

The micro-GA is based on the convergence of the micro-population towards a single individual representing the best result obtainable with that population. Once the convergence is reached, the best individual is preserved and the micro-population is restarted with new individuals. The definition of "the best individual" for each population is not easy in the case of multi-objective optimization, unless all objectives are combined in a single overall fitness function (see Senecal et al. [8-10]). In the approach followed in the present investigation, the three fitness functions were kept separated in the optimization process and individuals were compared with Pareto's criterion. This criterion leads to the definition of a number of non dominated individuals which can be higher than the number of objectives to be optimized, as illustrated in the example of Figure 1. Thus, the convergence of the micro-population towards a single individual could be meaningless for multi-objective optimization. Therefore, the effectiveness of micro-GA versus standard GA cannot be assessed "a priori" when the complexity of the optimization problem increases.

SELECTION OF THE BEST CONFIGURATIONS

From the results obtained with the optimization process, the five configurations (A, B, C, D, E of Figure 4) have been selected from Pareto's front. The performance of these chambers for the three operating modes of Table 1 are reported in Table 4.Even if the chambers of Table 4 give a significant improvement with respect to a particular operating condition, none of them can be said to be better than the baseline configuration for all operating modes and for all optimization goals. This comes as little surprise since the commercial combustion chamber, used as baseline case, has already been optimized for this kind of engine configuration and injection strategy.

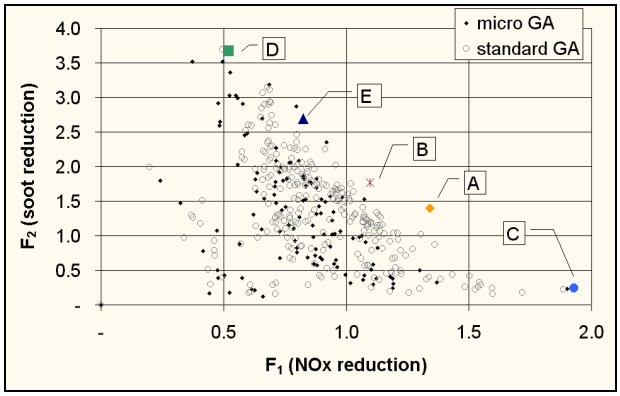

Figure 4 – Results of the optimization process

On the other hand, the results of Table 4 stress the importance of including several modes in the optimization process since the performance of each chamber is strongly affected by the operating conditions. Of course, the number of modes included in the optimization process could be increased so that the whole driving test could be considered but this would require a prohibitive computational time.

Configurations A and B present lower soot emissions than the baseline case for mode 1 and higher for mode 2, while chambers E performs better at the operating condition of mode 2. The effectiveness of these configurations at each operating condition can also be deduced by applying the merit function used by Reitz [8; 10] to the chambers of Table 4; in particular, configuration A should have a merit function 50% higher than the baseline one for mode 1, while for mode 2 the merit function is increased by 30% when moving from the baseline chamber to configuration E.

As far as the effect of combustion chamber geometry on engine emissions is concerned, NO_x levels seem less sensitive to combustion chamber geometry than soot, which shows changes of a factor 4 with respect to the baseline case. Moreover, NO_x emissions are less influenced by operating conditions. In fact, while it is possible to keep NO_x emissions low and almost constant over a wide range of operating conditions (see chamber C for mode 1 and 2, and mode 3), it was not possible to obtain the same result for soot. Note that HC and soot levels are optimized by the same combustion chamber shapes; thus the influence of the geometrical parameters on engine emissions will be analyzed only with reference to soot and NO_x emissions.

Chamber geometry	θ	Mode	NOx [g/kgf]	soot [g/kgf]	HC [g/kgf]	IMEP* [MPa]
Baseline 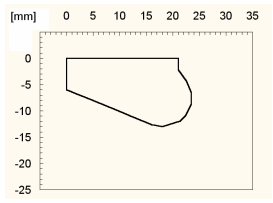	80	**1**	11.3	0.92	2.22	0.796
		2	21.0	0.49	0.8	1.211
		3	6.2	3.48	4.3	1.276
A 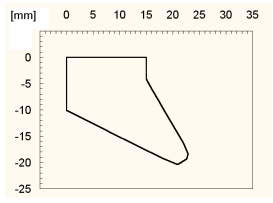	74	**1**	11.2	0.4	0.63	0.756
		2	12.3	1.0	0.38	1.118
		3	3.6	6.63	20.6	1.241
B 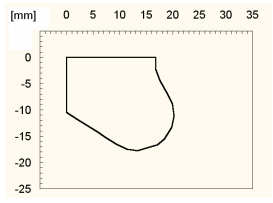	74	**1**	14.1	0.31	0.66	0.795
		2	14.9	0.84	0.70	1.162
		3	3.9	5.63	12.7	1.21
C 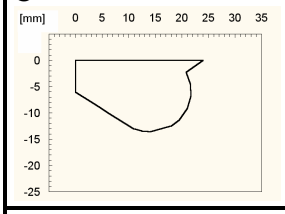	80	**1**	7.4	2.75	4.05	0.730
		2	8.3	2.83	2.4	1.124
		3	7.7	3.85	6.93	1.338
D 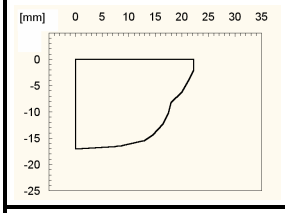	54	**1**	28.2	0.19	0.43	0.840
		2	32.9	0.19	0.54	1.269
		3	10.7	5.93	17.8	1.372
E 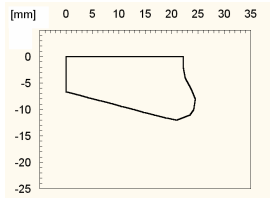	66	**1**	15.1	0.33	1.39	0.796
		2	23.3	0.19	0.7	1.226
		3	13.4	3.46	4.67	1.434

- The IMEP has been estimated by integrating $-pdV$ over the simulated portion of the engine cycle

Table 4 – Chamber geometry and predicted emissions for configurations A, B, C, D, E

INFLUENCE OF THE GEOMETRIC PARAMETERS ON SOOT AND NO_X EMISSIONS

The plots of Figure 5 and Figure 7 represent the influence of combustion chamber shape and spray angle on the reduction of NO_x and soot emissions for mode 1 and 2. The graphs in the upper side of Figure 5 and Figure 7 indicate the evolution of the ratio $NO_x/(NO_X)_0$ and the shape of the corresponding bowl geometry while on the bottom is reported the spray angle associated to that configuration.

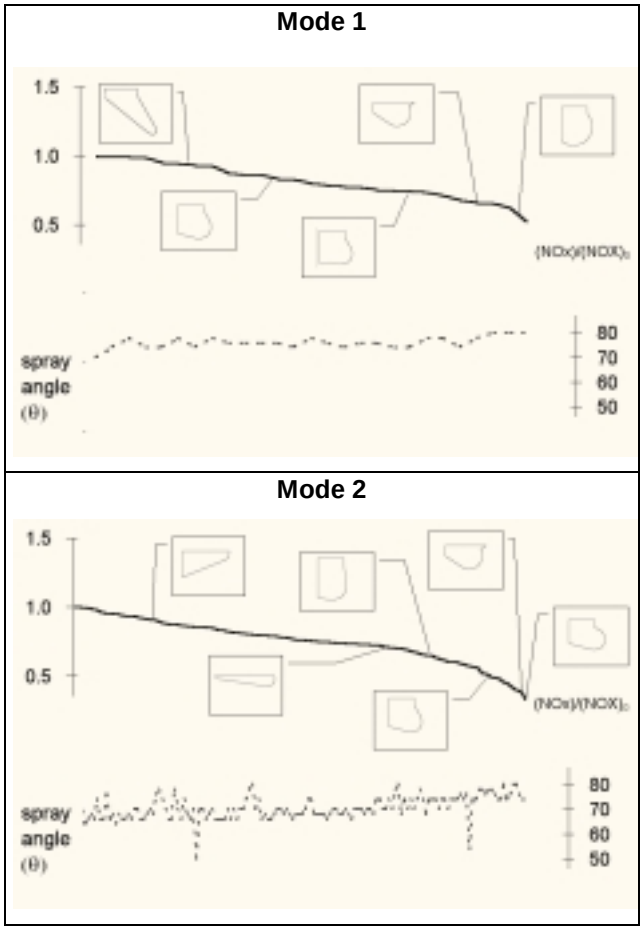

Figure 5 – Influence of combustion chamber on NO_x emissions

The NO_x reduction trends of the two modes confirm that this kind of pollutant emission is less influenced by the operating conditions since quite similar chambers are obtained for both modes. Note that chamber C of Table 4 strongly reduces NO_x emissions for the two conditions; however, other smaller-throat chambers perform better than configuration C. These chambers do not appear on Pareto's front of Figure 4 because they are characterized by very low IMEP values compared with the baseline case and with chamber C.

According to the results of Figure 5, the spray angle θ should be increased to reduce NO_x emissions in both operating conditions. This high values of the spray angle let the fuel to be injected inside the bowl flowing from top to bottom, thus confining most of the combustion phase into the bowl. Consequently, the combustion phase lays on the reach limit and, therefore, the concentration of oxygen in the high temperature zone is very low resulting in a reduced NO_x rate of formation. Furthermore, the configurations optimizing NO_x are characterized by a strong impingement on the walls of the bowl which reduces the air-fuel mixing; as a consequence, the premixed combustion phase is reduced and the low NO_x levels are often accompanied with lower in-cylinder average pressure levels. This is confirmed by the plots of Figure 6, where the mixture mass with an equivalence ratio greater than 1.5 is plotted together with the rate of heat release (ROHR) for mode 1 and chamber C and baseline configuration. Note that the larger quantity of mixture with Errore. Non si possono creare oggetti dalla modifica di codici di campo. produced with configuration C results in higher HC emissions with respect to the baseline case.

The throat radius x_e has an important effect on NO_x. In fact, because of the constant value of the bowl volume, low values of the throat radius result in a chamber geometry that better confines the combustion event. However, as load and speed increase the air in the bowl is not sufficient to allow a complete combustion and deep bowl are not adequate to keep the combustion confined. Therefore for mode 2 more shallow and reentrant bowl perform better. At the higher speed and load the re-entrance angle α tends to increase. For these conditions the bottom inclination parameter β decreases along the NO_x reduction trends. As a consequence of this the r parameter tends to be larger. The e_m parameter does not affect engine emissions.

To sum up, a narrow and deep combustion chamber with a shallow re-entrance and a low protuberance on the cylinder axis should be coupled with a spray oriented towards the bowl entrance to reduce NO_x emissions.

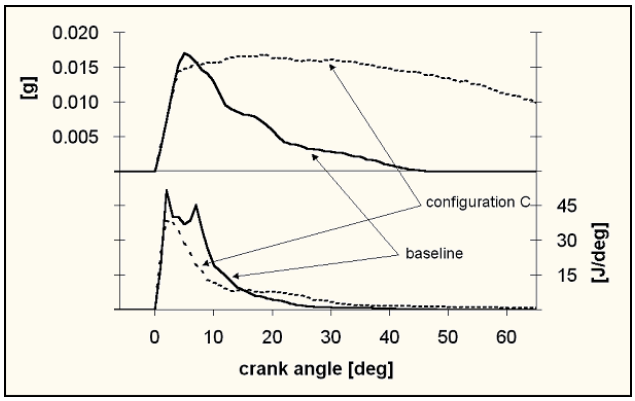

Figure 6 – Mixture fraction with ϕ>1.5 and ROHR for mode 1

As far as soot is concerned, all the chambers of Figure 7 are characterized by a large throat radius x_e (14% more than the baseline case) and a very small re-entrance, eventually becoming open chambers. Moreover, they are

characterized by a large toroid radius r while the inclination of the bowl bottom tends to be reduced up to flat-bottom or diamond-shape chambers.

However, the overall geometrical features necessary to reduce soot emissions are remarkably sensitive to operating conditions. Note that chamber D of Table 4 can be easily detected as a compromise between the configurations which better reduce soot levels for mode 1 and 2.

For both operating modes, the configurations optimized for soot reduction are characterized by small values of the spray angle, i.e., the spray is directed the bottom of the bowl. In this way combustion is not confined into the bowl and therefore the air-fuel mixing is facilitated. This results in a leaner combustion and in a faster soot oxidation rate.

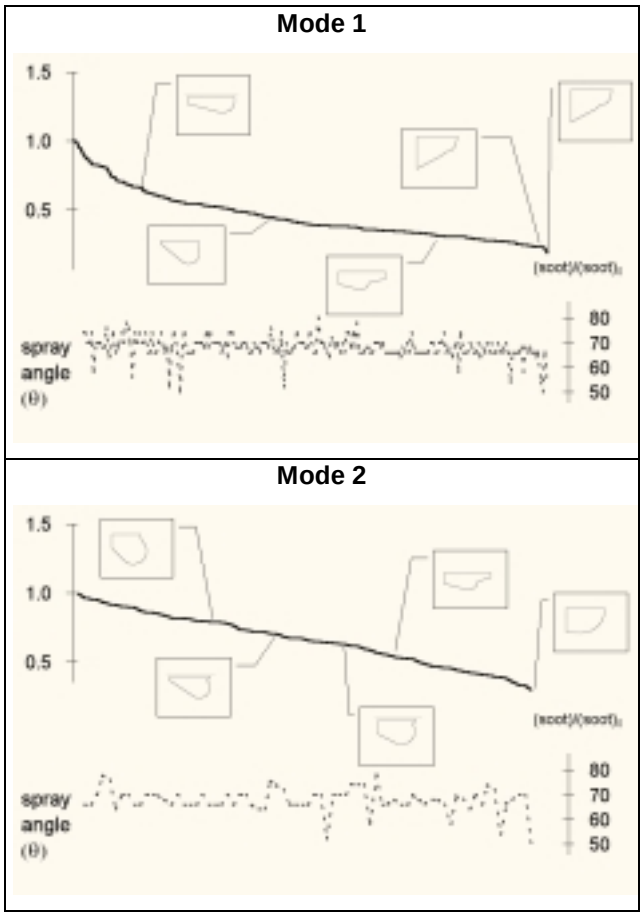

Figure 7 - Influence of combustion chamber on soot emissions

SUMMARY AND CONCLUSIONS

A multi-objective Genetic Algorithm has been applied to reduce diesel engine emissions in most recurring operating modes of the European Driving Test.

From the results of the optimization process, five configurations belonging to Pareto's front were selected and compared with the commercial chamber used as baseline case. Configurations A, B and E improved the overall engine emission for all the tested modes. Configurations C and D where found to reduce only NOx and Soot emissions, respectively.

Better results could be obtained by exploiting different injection strategies or changing other engine control parameters. On the other hand, by focusing the investigation on geometrical features only, one can put in evidence the influence of combustion chamber geometry on engine performance.

The analysis was performed separately for NO_x and soot emissions according to two modes, a low-speed low-load case (mode 1) and a medium-speed medium-load condition (mode 2). The following considerations were made:

→ For the same chamber, NO_x emissions are less influenced by engine operating conditions while the overall geometrical features necessary to reduce soot emissions are remarkably sensitive to load and speed values;

→ To reduce NO_x emissions, the combustion chamber should be narrow and deep with a shallow re-entrance and a low protuberance on the cylinder axis while the spray should be oriented towards the bowl entrance;

→ As far as soot is concerned, chambers characterized by a large throat radius x_e and a very small re-entrance were found; the inclination of the bowl bottom tends to be reduced up to flat-bottom (mode 2) or diamond-shape chambers (mode 1);

→ HC and soot levels are optimized by the same combustion chamber shapes.

ACKNOWLEDGMENTS

The financial support to this research was partially provided by the Italian Ministry for Instruction, University and Research (MIUR), lex 488/92 cluster 26 project P11.

REFERENCES

1. Hippolyt Saurer, *Improvements in and relating to Internal Combustion Engines of the Liquid Fuel Injection Type*, Patent N. GB421101, December 13th, 1934.
2. Lohr, J; Maschf Augsburg Nuerberg, *Air Compressiong Internal Combustion Engine with Direct Injection*, Patent N. US3814066, June 4th, 1974.
3. Neitz, A., D'Alfonso, N., " The M.A.N. Combustion System with Controlled Direct Injection for Passenger Car Diesel Engines", SAE paper 810479, 1981.

4. Heywood, J. B., *Internal Combustion Engine Fundamentals*- Mc Graw-Hill New York, 1988;

5. Tsao, K. C., Dong, Y., Xu, Y., “Investigation of Flow Field and Fuel Spray in a Direct-Injection Diesel Engine via Kiva-II Program”, SAE Paper 901616, 1990.

6. Zhang, L., Ueda, T., Takatsuki, T., Yokota, K., “A Study of the Effect of Chamber Geometries on Flame Behavior in a DI Diesel Engine” – SAE Paper No. 952515, 1995.

7. Bianchi, G.M., Pelloni, P., Corcione, F.E., Mattarelli, E., Luppino Bertoni, F., “Numerical Study of the Combustion Chamber Shape for Common Rail H.S.D.I. Diesel Engines”, SAE Paper 2000-01-1179, 2000.

8. Senecal, P.K., Reitz, R.D., "Simultaneous Reduction of Engine Emissions and Fuel Consumption using Genetic Algorithms and Multidimensional Spray and Combustion Modeling", SAE paper 2000-01-1890, 2000.

9. Senecal, P.K., Montgomery, D.T., Reitz, R.D., "Diesel Engine Optimization using Multi-Dimensional Modeling and Genetic Algorithms Applied to a Medium Speed, High Load Operating Condition", ASME-ICED 2000 Fall Technical Conference, 2000.

10. Wickman, D.D., Senecal, P.K., Reitz, R.D., "Diesel Engine Combustion Chamber Optimization Using Genetic Algorithms and Multi-Dimensional Spray and Combustion Modeling", SAE paper 2001-01-0547, 2001.

11. de Risi, A., Manieri, D., and Laforgia, D., ”A Theoretical Investigation on the Effects of Combustion Chamber Geometry and Engine Speed on Soot and NOX Emissions”, ASME-ICE, vol. 33-1, pp. 51-59, Book No. G1127A, 1999.

12. Senecal, P.K., Pomraning, E., Richards, K., “Multi-Mode Genetic Algorithm Optimization of Combustion Chamber Geometry for Low Emissions”, SAE paper 2002-01-0958.

13. Carroll, D.L., "Genetic Algorithms and Optimizing Chemical Oxygen-Iodine Lasers", Developments in Theoretical and Applied Mechanics, 18, 411, 1996.

14. Donateo, T., de Risi, A., and Laforgia, D., "Optimization of High Pressure Common Rail Electro-injector using Genetic Algorithms", SAE paper 2001-01-1980, 2001.

15. de Risi, A., Donateo, T., and Laforgia, D., "An application of Multi-Criteria Genetic Algorithms to the Optimization of a Common-Rail Injector”, ASME-ICE-Vol. 38, pp. 251-258, ASME Spring Technical Conference, 2002.

16. Carlucci, A. P., De Risi, A., Donateo, T., Ficarella, A., “A Combined Optimization Method for Common Rail Diesel Engines”, ASME-ICE-Vol. 38, pp. 243-250, ASME Spring Technical Conference, 2002.

17. Amsden, KIVA 3 – A KIVA Program with Block-Sructured Mesh for Complex Geometries, Los Alamos National Labs, 1989.

18. Donateo, T., de Risi, A., Laforgia, D., “ Theoretical Investigation on the Influence of Physical Parameters on Soot and NOx Engine Emissions”, ASME-ICE-Vol. 36-2, pp. 53-64, ASME ICE Spring Technical Conference, 2001.

19. Han, Z., Reitz, R. D., “Turbulence Modeling of Internal Combustion Engines Using RNG-k-e Models”, Combustion Science Technology, vol. 106, 1995, pp. 207.

20. Beale, J. C., Reitz, R.D., “Modeling Spray Atomization with the Kelvin-Helmoltz/Rayleigh Taylor Hybrid Model”, *Atomization and sprays*, Vol. 9, 1999, pp 623-650.

21. Halstead, M.P., Kirsch, A., Quinn, C.P., “The Autoignition of Hydrocarbon Fuels at High temperature and Pressure – Fitting of a Mathematical Model”, *Combustion and Flame*, 30, 1997, pp.45-60.

22. Abraham, J., Bracco, F.V., Reitz. R.D., “Comparison of Computed and Measured Premixed Charge Engine Combustion”, *Combustion and Flame*, 60, 1985, pp 309-322.

23. Hiroyasu, H., Nishida, K., "Simplified Three Dimensional Modeling of Mixture Formation and Combustion in a D.I. Diesel Engine", SAE Paper 890269;

24. Nagle, J., Strickland-Constable, R. F., “Oxidation of Carbon between 1000-2000 °C”, Procedure of the Fifth Carbon Conference, Vol. 1, Pergammon Press, 1962.

25. De Risi, A., Donateo, T., Laforgia, D., “Theoretical Investigation on Variable Density Sprays”, *Atomization and sprays*, Vol 12, 2002, pp.329-358.